

Supplementary Information

Surface modification of MoO_xS_y on porous TiO_2 nanospheres as an anode material with highly reversible and ultra-fast lithium storage properties

Yun Qiao,^a Xianluo Hu,*^a Yang Liu,^a Gan Liang,^b Mark C. Croft,^c and Yunhui Huang*^a

^a State Key Laboratory of Material Processing and Die & Mould Technology, School of Materials Science and Engineering, Huazhong University of Science and Technology, Wuhan 430074, P. R. China.

^b Department of Physics, Sam Houston State University, Huntsville, Texas 77341, USA.

^c Department of Physics and Astronomy, Rutgers University, Piscataway, New Jersey 08854, USA.

* Corresponding author

E-mail: huxl@mail.hust.edu.cn; huangyh@mail.hust.edu.cn.

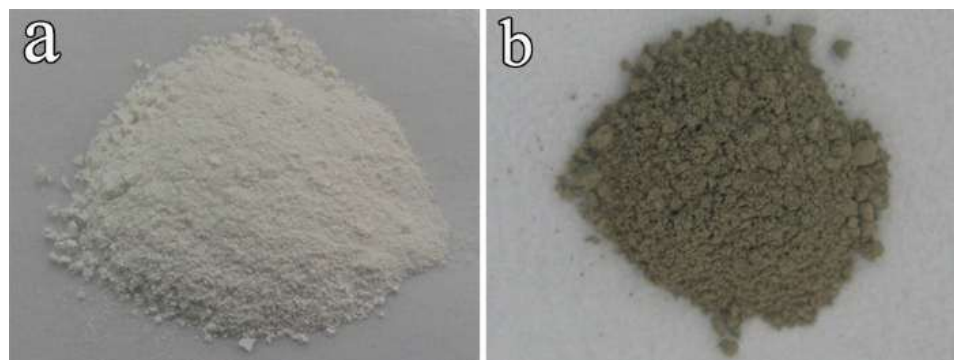


Fig. S1 Digital photos for nanoporous TiO₂ spheres (a) and TiO₂@MoO_xS_y nanocomposite (b).

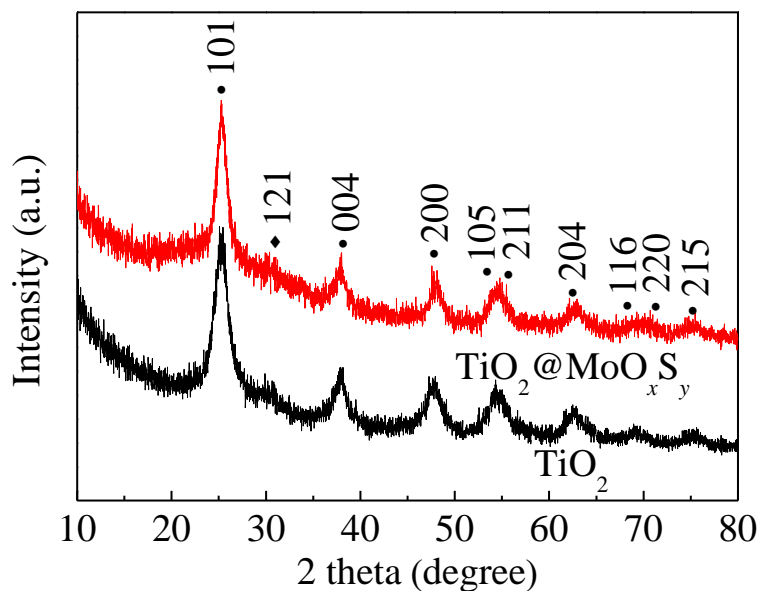


Fig. S2 XRD patterns of the nanoporous TiO₂ spheres and TiO₂@MoO_xS_y nanocomposite (◆brookite, • anatase).

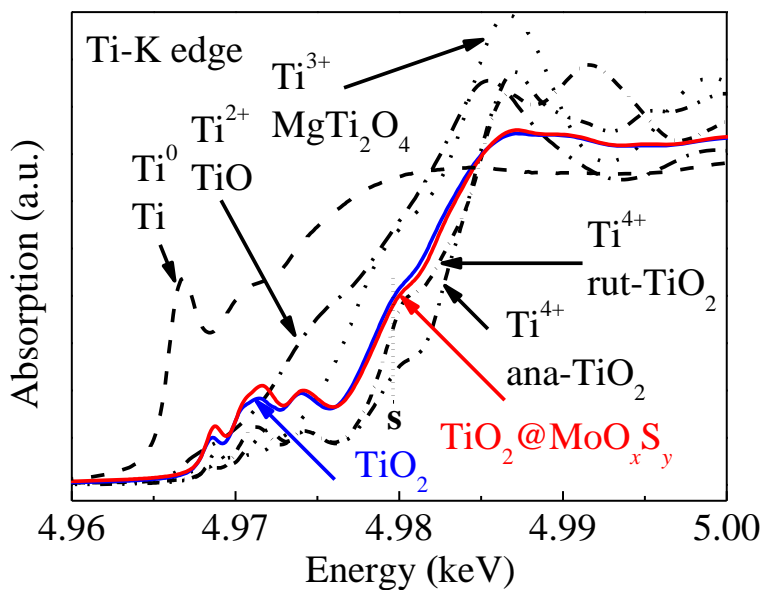


Fig. S3 XAS spectra of nanoporous TiO_2 spheres and $\text{TiO}_2 @ \text{MoO}_{x,y}$ nanocomposite collected at Ti K-edge.

In Figure S3, the Ti-K edges of nanoporous TiO_2 spheres and $\text{TiO}_2 @ \text{MoO}_{x,y}$ nanocomposites are presented along with a series of standard compound spectra. The first point to be noted is that the spectra are so nearly identical that they will be discussed here as being the same. The well-known chemical shift to higher energy, of the steeply rising main-edge, with increasing Ti valence is clear from the standard spectra. There are three typical octahedrally coordinated TiO_2 allotropes with different numbers of edge sharing octahedra: anatase (with 4), rutile (with 2), and brookite (with 3). Figure S3 displays the Ti-K edges of the first and second most common allotropes, anatase and rutile.^{1,2} Both of these standard phases are, of course, Ti^{4+} compounds with the apparent displacement of the anatase spectrum at the absorption coefficient level of ~0.5 to higher energy being associated with the low intensity of the s-shoulder-feature (as indicated in this figure). A brookite phase spectrum (see Figure 2a in the main article) manifests a strong s-feature similar to the rutile standard spectrum.^{1,3} The two spectra manifest a chemical shift typical of Ti^{4+} compounds with a robust intensity in the s-feature.

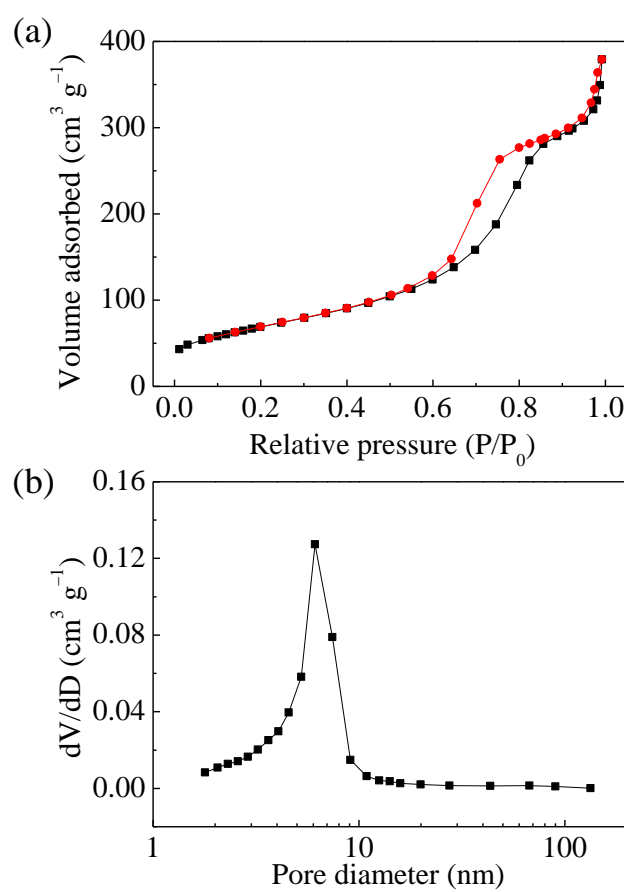


Fig. S4 (a) Nitrogen adsorption-desorption isotherm (b) and pore size distribution plot of the as-formed $\text{TiO}_2@\text{MoO}_x\text{S}_y$ nanocomposite.

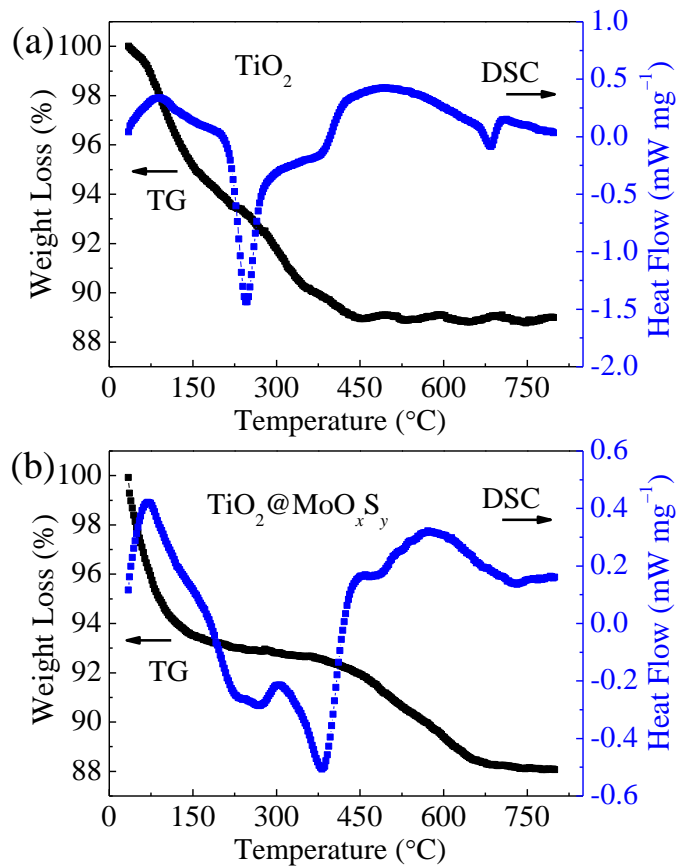


Fig. S5 TG/DSC analyses of nanoporous TiO_2 spheres (a) and $\text{TiO}_2 @ \text{MoO}_x\text{S}_y$ nanocomposite (b) measured at a heating rate of $10\text{ }^\circ\text{C min}^{-1}$ in a flowing air.

For nanoporous TiO_2 (Figure S5a), the exothermic peak appeared at around $250\text{ }^\circ\text{C}$, which might be assigned to the decomposition of the existence organic species. However, there is an extra exothermic peak at approximately $400\text{ }^\circ\text{C}$ for the $\text{TiO}_2 @ \text{MoO}_x\text{S}_y$ nanocomposite, which can probably be attributed to the oxidation of MoO_xS_y to MoO_3 (Figure S5a).^{4,5} By assuming that the surface coating product is MoS_2 and the remaining product is pure MoO_3 , which has a weight percentage of approximately 0.93%, it can be estimated that the MoO_xS_y content in the $\text{TiO}_2 @ \text{MoO}_x\text{S}_y$ nanocomposite is approximately 1.03%.⁵

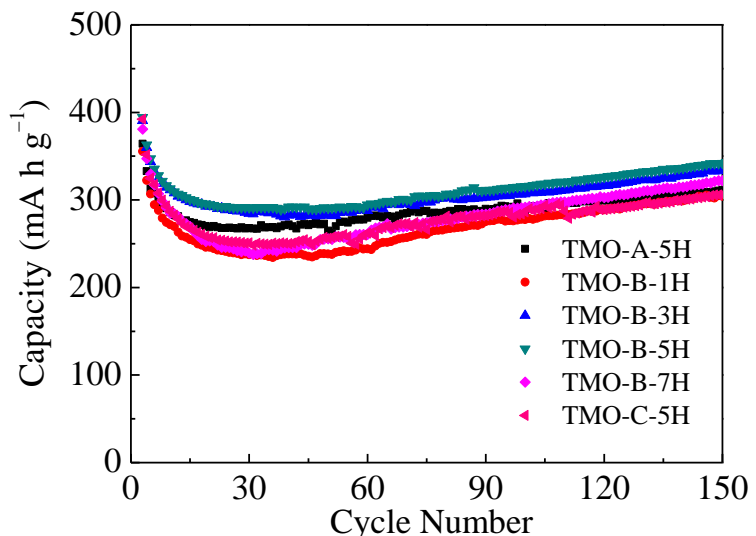


Fig. S6 Cycling performances of the $\text{TiO}_2@\text{MoO}_x\text{S}_y$ composites obtained under different conditions.

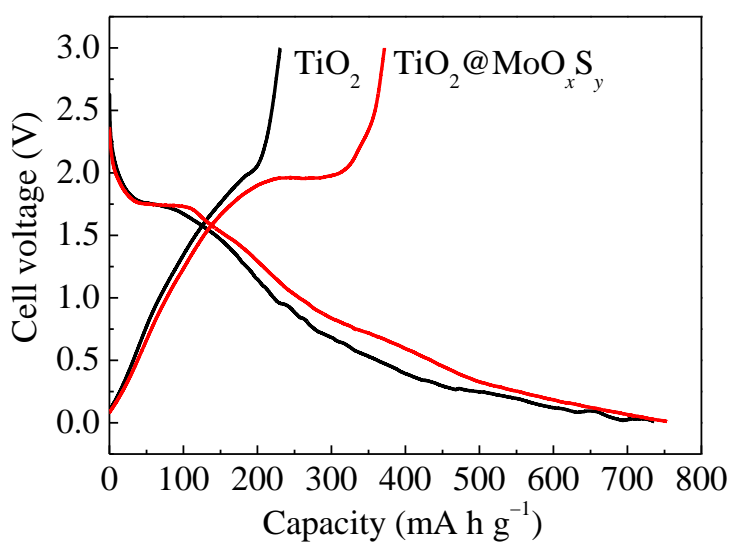


Fig. S7 Charge/discharge profiles of the initial cycle at a current density of 0.1 A g^{-1} of the electrodes made of the pure porous TiO_2 nanospheres and the as-formed $\text{TiO}_2@\text{MoO}_{x-y}\text{S}_y$ hybrid within a cut-off voltage window of 0.01–3.0 V.

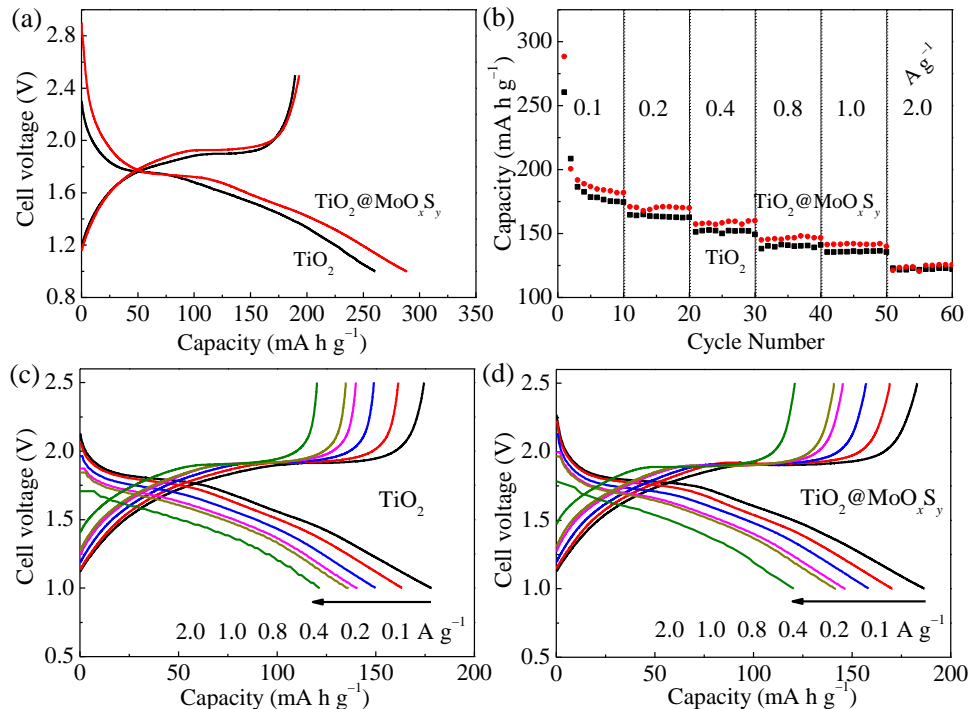


Fig. S8 Electrochemical performances of nanoporous TiO_2 spheres and $\text{TiO}_2@\text{MoO}_{x,y}$ nanocomposite within a cut-off voltage window of 1.0–2.5 V. (a) Charge/discharge profiles for the first cycle at a current density of 0.1 A g^{-1} . (b) Capacity retention at various current rates. (c, d) Charge-discharge profiles of nanoporous TiO_2 spheres and $\text{TiO}_2@\text{MoO}_{x,y}$ nanocomposite at different discharge current rates, respectively (the 5th cycle at each current density).

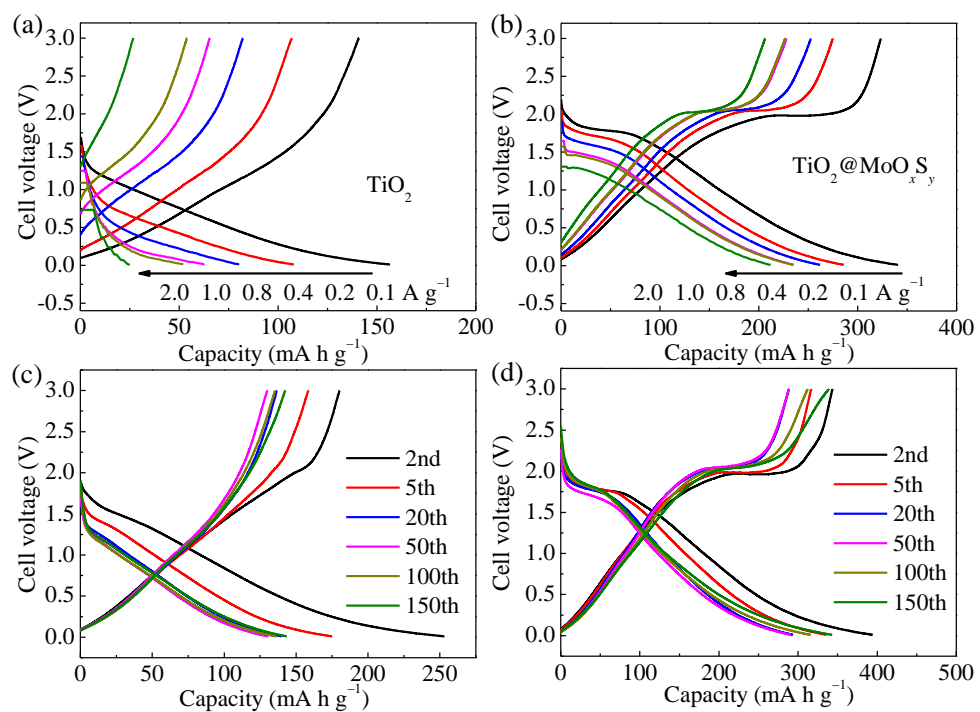


Fig. S9 Electrochemical performances of nanoporous TiO_2 spheres and $\text{TiO}_2@\text{MoO}_{x,y}$ nanocomposite within a cut-off voltage window of 0.01–3.0 V. (a, b) Charge-discharge profiles of nanoporous TiO_2 spheres and $\text{TiO}_2@\text{MoO}_{x,y}$ nanocomposite at different discharge current rates, respectively (the 5th cycle at each current density). (c, d) Discharge/charge profiles of nanoporous TiO_2 spheres and $\text{TiO}_2@\text{MoO}_{x,y}$ nanocomposite at a current density of 0.1 A g^{-1} , respectively.

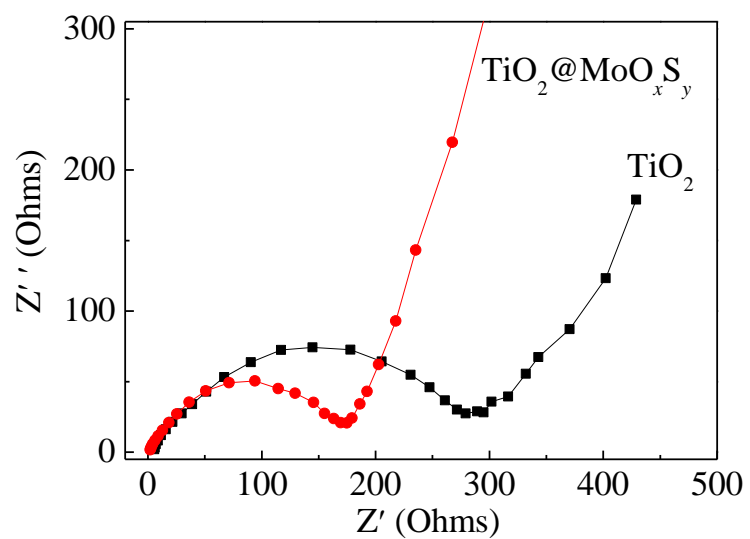


Fig. S10 Electrochemical impedance spectra of the electrodes made of the pure porous TiO_2 nanospheres and the as-formed $\text{TiO}_2\text{@MoO}_x\text{S}_y$ hybrid within a cut-off voltage window of 0.01–3.0 V.

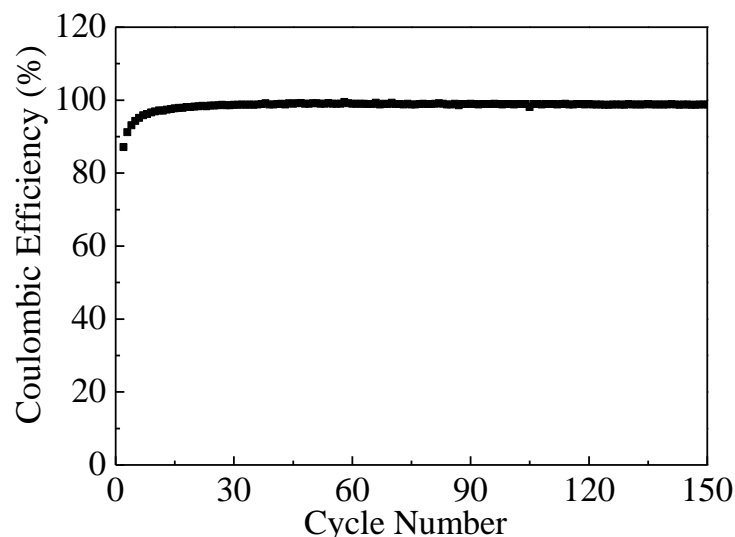


Fig. S11 The coulombic efficiency of the as-formed $\text{TiO}_2@\text{MoO}_x\text{S}_y$ hybrid at a current density of 0.1 A g^{-1} .

References:

- 1 P. C. Angelomé, L. Andrini, M. E. Calvo, F. G. Requejo, S. A. Bilmes and G. J. A. Soler-Illia. *J. Phys. Chem. C*, 2007, **111**, 10886-10893.
- 2 R. B. Greegor, F. W. Lytle, R. C. Ewing and K. Keil. in *Lunar and Planetary Institute Science Conference Abstracts*. 257-258.
- 3 Farrel Lytle section of the IXAS XAFS database.
http://ixs.iit.edu/database/data/Farrel_Lytle_data/RAW/Ti/index.html.
- 4 S. Ding, J. S. Chen and X. W. Lou. *Chem. Eur. J.*, 2011, **17**, 13142-13145.
- 5 S. M. Paek, H. Jung, M. Park, J. K. Lee and J. H. Choy. *Chem. Mater.*, 2005, **17**, 3492-3498.